

Two transitions in tangentially anchored nematic droplets

This content has been downloaded from IOPscience. Please scroll down to see the full text.

1986 J. Phys. A: Math. Gen. 19 3211

(<http://iopscience.iop.org/0305-4470/19/16/019>)

View [the table of contents for this issue](#), or go to the [journal homepage](#) for more

Download details:

IP Address: 131.215.114.240

This content was downloaded on 24/10/2013 at 17:32

Please note that [terms and conditions apply](#).

Two transitions in tangentially anchored nematic droplets

R D Williams

Rutherford Appleton Laboratory, Chilton, Didcot, Oxon OX11 0QX, UK

Received 9 December 1985

Abstract. In an axisymmetric approximation we demonstrate a parity breaking transition to a twisted configuration in tangentially anchored nematic liquid crystal droplets. The twisted phase occurs when $K_{11} \geq K_{22} + 0.431 K_{33}$. In a magnetic field there is another transition corresponding to the droplet axis changing from parallel to normal to the field.

1. Introduction

A nematic liquid crystal is anisotropic, for the rodlike molecules are on average parallel to a unit vector \mathbf{n} . On macroscopic scales, \mathbf{n} is a continuous field $\mathbf{n}(\mathbf{x})$, and an elastic energy density is associated with the squares of gradients of \mathbf{n} . Thus the elastic energy of a volume of nematic is proportional to the linear dimension L of the volume. For a compact volume, such as a drop of nematic suspended in isotropic fluid, there is also surface energy, proportional to L^2 . Thus the internal energy of a large drop is dominated by the surface energy, and so the drop is spherical. At the nematic surface, there is energy per unit area associated with deviations of the anchoring angle from the easy angle [1]. By the same dimensional reasoning as above (given more explicitly in § 2 and the appendix) the anchoring angle is always the easy angle: so-called strong anchoring. Furthermore, spherical drops and strong anchoring hold for drops larger than a few microns in size.

If the director at the surface is normal to the surface, the director points radially from the centre of the sphere, with perhaps a twist [2]. If the easy angle is between 0 and 90° (conical boundary conditions), then the positions of the singularities in \mathbf{n} change continuously with the elastic constants and also with the easy angle [3]. Furthermore, there are problems from the sign ambiguity of \mathbf{n} , which arise for the following reason. Although the ends of a nematogen molecule are in general different, the energy difference between a parallel and an antiparallel pair is much smaller than the temperature, so ordering in direction \mathbf{n} is physically the same as ordering in direction $-\mathbf{n}$. Alternatively, the energy difference may be large and stable antiparallel pairs can form, in which case \mathbf{n} is also equivalent to $-\mathbf{n}$ because the pairs are symmetric. Thus there may be 'branch-cut surfaces' across which \mathbf{n} changes sign. If one of these surfaces is bounded in part by the surface of the sphere and in part by a line disclination, then it cannot be removed, only moved. This is analogous to the representation of an angle by a real number: the number can have discontinuities of 2π even though the underlying angle is continuous.

The situation is considerably simpler when the director is tangential to the surface. The bipolar configuration, suggested by Chandrasekhar [4] and Dubois-Violette and Parodi [5], seems to be adopted by many nematics. The director is parallel to curves

which join two diametrically opposite points of the surface of the drop, these curves lying on planes of constant azimuth. Twisted bipolar configurations (cf figure 2) have been observed [3], with the limiting case of these twisted drops where the director is in the azimuthal direction like the magnetic field of a straight wire: we call this the 'toroidal' configuration.

In this paper we examine tangentially anchored nematic drops, using the topology of the untwisted bipolar configuration, but with varying amounts of twist in the director field. We find that when the splay constant is small, the droplet is untwisted and when the splay constant is large, the droplet is twisted.

Since nematogen molecules tend to be parallel to a magnetic field, we expect the axis of an untwisted drop (when the splay constant is small) to be parallel to the field, and that of a very twisted toroidal drop perpendicular. There is a second-order transition between these phases, associated with a breaking of axial symmetry.

In the following, we use the three-term Frank energy and justify the neglect of the fourth (surface) term in view of the tangential anchoring assumption; a more general formulation of the Frank energy can be found in [6]. We use a local surface-anchoring energy; a more general treatment of liquid crystal surfaces can be found in [7].

2. Theory

Let V_0 be a volume of nematic liquid crystal, which can be considered as a fiducial volume V multiplied by a length scale R . Later V will be the unit sphere and V_0 a sphere of radius R .

A unit-vector field $\mathbf{n}(\mathbf{x})$, $\mathbf{x} \in V$, is the scaled director field. The equilibrium shape and director for given R are obtained by minimising the elastic energy, which is a sum of a volume and a surface energy. The volume energy is the Frank elastic energy [8], which is a sum of contributions from splay, bend and twist, each with an associated elastic constant, which we shall call $K_{11} = K$, $K_{33} = K\kappa_B$, $K_{22} = K\kappa_T$, respectively. Since the Frank energy is a volume integral of squares of gradients of \mathbf{n} , K must have dimensions of force. We can thus write the Frank energy as $\pi KRu[\mathbf{n}]$ where the factor π has been removed for later convenience, and

$$u[\mathbf{n}] = (1/\pi) \int_V F(\mathbf{n}, \nabla \mathbf{n}) \, d\mathbf{x} \quad (2.1)$$

$$F = \frac{1}{2}(\text{div } \mathbf{n})^2 + \frac{1}{2}\kappa_B(\mathbf{n} \times \text{curl } \mathbf{n})^2 + \frac{1}{2}\kappa_T(\mathbf{n} \cdot \text{curl } \mathbf{n})^2. \quad (2.2)$$

The surface energy may be written as

$$\pi WR^2 \int_S f(\mathbf{n} \cdot \mathbf{k}) \, d\mathbf{x} \quad (2.3)$$

where S is the surface of V , W is a constant with the dimensions of surface tension and f is a dimensionless function of the angle between the director and the surface normal \mathbf{k} . The angle corresponding to the minimum of f is the easy angle [1] and W times the second derivative of f at the easy angle is a measure of the anchoring energy coefficient [1]. With no loss of generality, we can adjust f to make W exactly the anchoring energy coefficient.

The quantity to be minimised is then the sum of volume and surface energies, which we can write as $\pi KRu_\mu[\mathbf{n}]$, where

$$u_\mu[\mathbf{n}] = u[\mathbf{n}] + \mu \int_S f(\mathbf{n} \cdot \mathbf{k}) \, dx \tag{2.4}$$

where $\mu = WR/K$. To keep \mathbf{n} unit we introduce two Lagrange multiplier fields, one for volume and one for surface, and thus define

$$\bar{u}_\mu[\mathbf{n}] = u_\mu[\mathbf{n}] - \frac{1}{2} \int_V \lambda(\mathbf{x})n^2 \, dx - \frac{1}{2} \int_S \Lambda(\mathbf{x})n^2 \, dx \tag{2.5}$$

which gives the Euler-Lagrange equations

$$\frac{\partial F}{\partial n_i} - \frac{\partial}{\partial x_j} \left(\frac{\partial F}{\partial n_{i,j}} \right) = \lambda n_i \tag{2.6}$$

$$k_j \frac{\partial F}{\partial n_{i,j}} + \mu k_i f'(\mathbf{n} \cdot \mathbf{k}) = \Lambda n_i \tag{2.7}$$

where (2.6) is true in the bulk and (2.7) on the surface. Taking (2.7) in the directions \mathbf{n} and \mathbf{k} allows elimination of Λ , and another equation is from the direction $\mathbf{n} \times \mathbf{k}$:

$$\text{div } \mathbf{n} + \mu f'(\mathbf{n} \cdot \mathbf{k}) + \frac{\mathbf{n} \cdot \mathbf{k}}{1 - (\mathbf{n} \cdot \mathbf{k})^2} \kappa_B[\mathbf{k}, \mathbf{n}, \text{curl } \mathbf{n}] = 0 \tag{2.8a}$$

$$\kappa_T(\mathbf{n} \times \mathbf{k})^2(\mathbf{n} \cdot \text{curl } \mathbf{n}) = \kappa_B(\mathbf{n} \cdot \mathbf{k})[(\mathbf{n} \times \mathbf{k}) \cdot (\mathbf{n} \times \text{curl } \mathbf{n})]. \tag{2.8b}$$

We wish to simplify the problem by removing these complicated surface boundary conditions and removing the necessity to minimise over droplet *shapes*. If $\mu = WR/K$ is large, the boundary condition (2.8) becomes simply $f'(\mathbf{n} \cdot \mathbf{k}) = 0$, which is the *strong anchoring regime*. Elastic constants for short-rod nematics are in the range 10^{-6} dyn [8] and a recent measurement of the anchoring coefficient for a nematic/liquid interface shows that W is of the order 10^{-3} dyn cm^{-1} [1]. Thus μ can be considered large when $R \geq 10 \mu\text{m}$. Droplets measured in [3] are about $30 \mu\text{m}$ in radius, so it is not grossly wrong to consider μ large. Even with strong anchoring, however, it is not clear that the surface energy contribution is small; but for tangential anchoring, when $f'(0) = 0$, it is shown in the appendix that for $\mu \rightarrow \infty$, the minimum of the total energy $u_\mu[\mathbf{n}]$ is the same as the minimum of the Frank energy $u[\mathbf{n}]$ with the restriction $\mathbf{n} \cdot \mathbf{k} = 0$ at the boundary. Given $\mathbf{n} \cdot \mathbf{k} = 0$, the surface tension must be constant, so the drop must be spherical. We take the volume V to be the unit sphere. For tangential anchoring and large drops, the boundary conditions are then

$$\begin{aligned} \mathbf{n} \cdot \mathbf{k} &= 0 \\ \mathbf{n} \cdot \text{curl } \mathbf{n} &= 0. \end{aligned} \tag{2.9}$$

We should mention at this point two additional contributions to the bulk Frank-Oseen energy, both of which are usually ignored because they can be written as surface terms. Here we are considering the surface terms explicitly and shall show that in the tangentially anchored case they can also be ignored. The additions can be written [6]

$$K_{15} \nabla \cdot (\mathbf{n} \nabla \cdot \mathbf{n}) - (K_{22} + K_{24}) \nabla \cdot (\mathbf{n} \nabla \cdot \mathbf{n} - (\mathbf{n} \cdot \nabla) \mathbf{n}). \tag{2.10}$$

The first term, the so-called Nehring-Saupe term, and also the first part of the second term, is a surface integral of $(\mathbf{n} \cdot \mathbf{k})(\nabla \cdot \mathbf{n})$ and $\mathbf{n} \cdot \mathbf{k} = 0$ for tangential anchoring. The

first part of the second term involves $\int dS \mathbf{k} \cdot [(\mathbf{n} \cdot \nabla) \mathbf{n}]$ which for tangential \mathbf{n} is simply $4\pi R$, and is an additive constant to the total energy.

The energy functional is a sum of splay, bend and twist contributions:

$$u[\mathbf{n}] = u_s[\mathbf{n}] + \kappa_B u_B[\mathbf{n}] + \kappa_T u_T[\mathbf{n}]. \quad (2.11)$$

We expect each of these three terms to contribute about equally, so that a small splay (bend, twist) constant is associated with a large $u_s(u_B, u_T)$, in the same way that any small elastic modulus causes a large distortion.

Experimental studies indicate that tangential boundary conditions imply the bipolar configuration: there is a singularity at diametrically opposite points of the surface (the 'poles'), with the director locally pointing radially away from each singularity. Under some conditions [5, 9, 10] the director field lines are planar or the parity symmetry may be broken, giving a twisted appearance to the drop [2] (cf figures 2(b) and (c)). We have calculated numerically [11] the director field with the one-constant approximation $\kappa_B = \kappa_T = 1$, and no other approximation, and the drop has the appearance shown in figure 1. It can be seen that circles (overdrawn in figure 1) which pass through both poles are a good approximation to the field lines. It is for this reason that we use an orthogonal coordinate system tailor-made for the singularities of the problem.

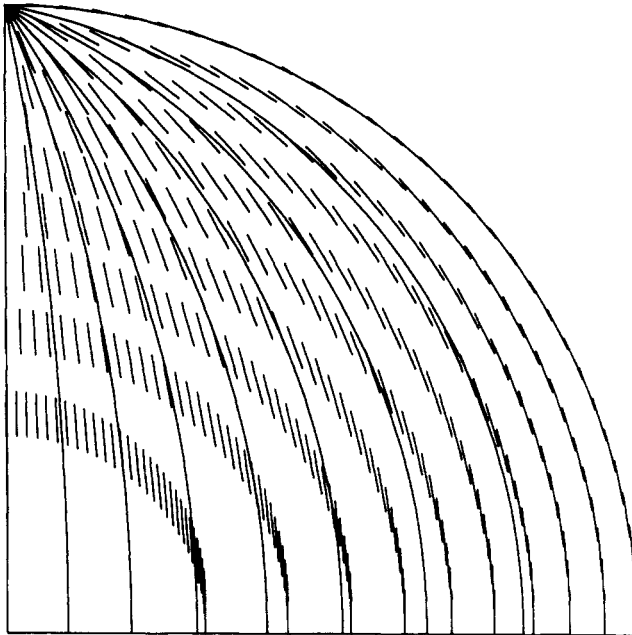


Figure 1. Exact director configuration in the one-constant approximation, from [9], with overlaid circles to show accuracy of fit.

Bispherical coordinates (ξ, η, ϕ) consist of two poles a distance 2 apart connected by an axis of cylindrical symmetry, which is associated with the angle ϕ . Part of a plane of constant ϕ is illustrated in figure 2(a). The lines of constant η are circles passing through both poles and the orthogonal set of constant ξ are also circles. The transformation to cylindrical coordinates (x, r, ϕ) measured from an origin midway

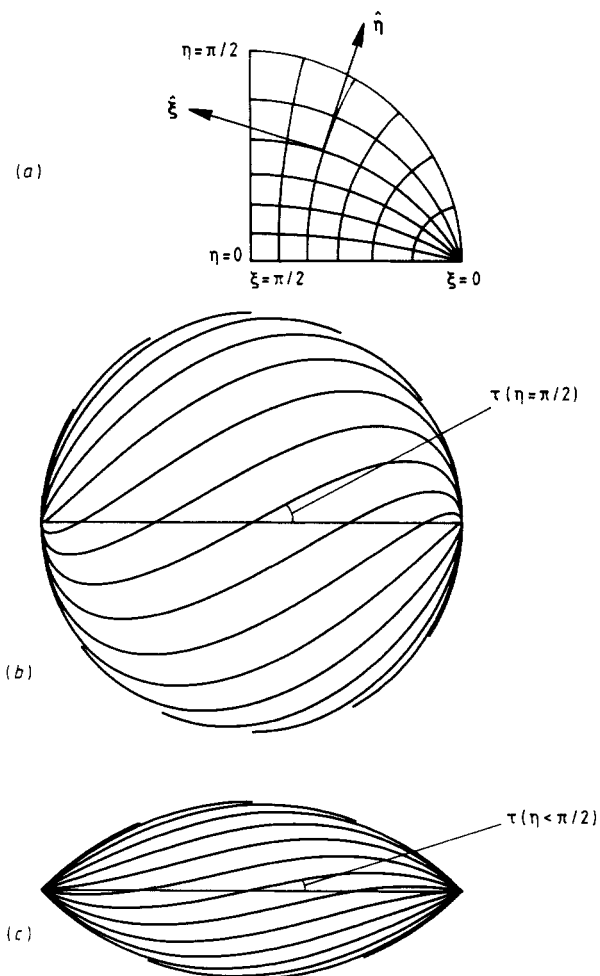


Figure 2. (a) Bispherical coordinate system with unit vectors. The vector ϕ is normal to the paper. (b) Director field lines for $\tau(\pi/2) = 29^\circ$. (c) Field lines for $\eta = 25^\circ$, $\tau(\eta) = 22^\circ$.

between the poles is

$$\begin{aligned} x &= Z^{-1} \cos \xi \\ r &= Z^{-1} \sin \xi \sin \eta \end{aligned} \tag{2.12}$$

where

$$Z = 1 + \sin \xi \cos \eta.$$

The quadrant in figure 2(a) is the area $0 \leq \xi \leq \pi/2, 0 \leq \eta \leq \pi/2$, and the metric elements $h_\xi = ds/d\xi$, etc, are given by

$$\begin{aligned} h_\xi &= Z^{-1} \\ h_\eta &= Z^{-1} \sin \xi \\ h_\phi &= Z^{-1} \sin \xi \sin \eta. \end{aligned} \tag{2.13}$$

We now assume the director to have no $\hat{\eta}$ component, which we justify by looking at figure 1, and write

$$\mathbf{n} = \hat{\xi} \cos[\tau(\eta)] + \hat{\phi} \sin[\tau(\eta)] \tag{2.14}$$

where $\hat{\xi}, \hat{\eta}, \hat{\phi}$ is the triad of unit vectors and the angle τ is the twist angle. A field line remains on a surface of constant η and ends at each of the poles and makes a constant angle with planes through the poles. The surface $\eta = \pi/2$ is a sphere which is the surface of the drop, so the tangential anchoring condition is satisfied. Figure 2(b) illustrates the field lines on the surface of the drop and figure 2(c) shows them on an interior surface. Using the ansatz (2.14) and the divergence theorem, after some algebra we find

$$u_s = \int dV \frac{1}{2}(\text{div } \mathbf{n})^2 = 4\pi \int_0^{\pi/2} \frac{d\eta}{\sin^2 \eta} (\eta - \cos \eta \sin \eta) \cos^2 \tau \tag{2.15a}$$

$$u_T = \int dV \frac{1}{2}(\mathbf{n} \cdot \text{curl } \mathbf{n})^2 = 2\pi \int_0^{\pi/2} d\eta \eta (d\tau/d\eta + \sin \tau \cos \tau \cot \eta)^2 \tag{2.15b}$$

$$\begin{aligned} u_B &= \int dV \frac{1}{2}(\mathbf{n} \times \text{curl } \mathbf{n})^2 \\ &= \pi \int_0^{\pi/2} d\eta \left(\frac{\eta}{\sin^2 \eta} (1 + \sin^2 \tau + 2 \cos^2 \eta \cos^4 \tau) - 3 \cot \eta \cos^2 \tau \right). \end{aligned} \tag{2.15c}$$

It can be seen that the twist and bend energies are logarithmically infinite at the axis ($\eta \rightarrow 0$) unless $\tau \rightarrow 0$. If (x, r, ϕ) is the cylindrical coordinate system, the director field must be $\mathbf{n} = \hat{x}$ at the axis. An infinite splay energy $\mathbf{n} = \hat{r}$ will escape by converting to finite splay and finite bend energy [8], and an infinite bend energy $\mathbf{n} = \hat{\phi}$ will escape by converting to finite bend and finite twist energy [12]. Here we have the latter. Indeed, for small bend constant we expect the drop to have $\mathbf{n} = \hat{\phi}$ everywhere except near the axis, where there is a twist relaxation—this limit we call the *toroidal* configuration. The condition $\mathbf{n} = \hat{x}$, together with $\mathbf{n} \cdot \text{curl } \mathbf{n} = 0$ on the surface (cf (2.9)), give the boundary conditions for $\tau(\eta)$:

$$\begin{aligned} \tau(0) &= 0 \\ d\tau/d\eta|_{\eta=\pi/2} &= 0. \end{aligned} \tag{2.16}$$

The director configuration $\tau(\eta)$ is obtained by minimising the sum of the splay, twist and bend energies (2.15a, b, c) respectively. The Euler-Lagrange equation is

$$\begin{aligned} 4\kappa_T \left(\eta \frac{d^2 \tau}{d\eta^2} + \frac{d\tau}{d\eta} \right) \\ = \sin 2\tau [(4 - 2\kappa_T + 3\kappa_B) \cot \eta + (-4 + 2\kappa_T + \kappa_B) \eta \text{cosec}^2 \eta \\ + 2\eta \cot^2 \eta (\kappa_T - 2\kappa_B \cos^2 \tau)]. \end{aligned} \tag{2.17}$$

One solution is $\tau(\eta) = 0$, corresponding to the parity symmetric untwisted drop, with energy

$$u[\mathbf{n}] = u_s + \kappa_B u_B = 4 + \kappa_B (3 - \pi^2/4) \tag{2.18}$$

which has no dependence on the twist elastic constant. The ratio u_s/u_B is 7.5, so we expect this solution to be the absolute minimum when the bend constant is large.

In the rest of this section, we make some analytic estimates of the solution $\tau(\eta)$ and in § 3 we shall calculate it numerically.

We can calculate the energy $u[\mathbf{n}]$ when τ is slightly different from zero, by linearising the Euler-Lagrange equation, and solve the resulting Sturm-Liouville problem, to obtain a set of eigenfunctions $\tau_i(\eta)$ with eigenvalues λ_i such that for small deviations from $\tau = 0$:

$$u\left(\sum_i c_i \tau_i(\eta)\right) = \sum_i \lambda_i c_i^2. \tag{2.19}$$

When these eigenvalues are all positive, the solution $\tau(\eta) = 0$ is stable, and if the transition is second order, the line $\min\{\lambda_i\} = 0$ in the (κ_B, κ_T) plane separates the parity symmetric bipolar phase from the twisted phase. The lowest- λ eigenfunction will have no nodes and will satisfy the boundary conditions (2.16), so we approximate it by $\sin \eta$, in which case the energy can be calculated and we find that the untwisted drop is realised when

$$\kappa_B \geq (1 - \kappa_T) \frac{4\pi^2 - 16}{20 - \pi^2} \sim 2.32(1 - \kappa_T) \tag{2.20}$$

so that for large κ_B and for large κ_T the untwisted configuration is the minimum energy.

The only dependence on $d\tau/d\eta$ in the energy functional occurs in the twist energy. Thus when $\kappa_T = 0$, the energy minimisation can be done separately at each value of η ; the splay and bend energies are quadratic in $\sin^2 \tau$, which can be minimised immediately:

$$\sin^2[\tau(\eta)] = \frac{1}{\kappa_B} \left(\sec^2 \eta - \frac{\tan \eta}{\eta} \right) + 1 - \frac{3 \tan \eta}{4\eta} - \frac{\sec^2 \eta}{4}. \tag{2.21}$$

When this expression is less than zero or greater than 1, τ is 0 or $\pi/2$ respectively. When η is close to its limits,

$$\begin{aligned} \sin^2 \tau &\rightarrow \left(\frac{2}{3\kappa_B} - \frac{1}{2} \right) \eta^2 && \eta \rightarrow 0 \\ \sin^2 \tau &\rightarrow \left(\frac{1}{\kappa_B} - \frac{1}{4} \right) (\pi/2 - \eta)^{-2} && \eta \rightarrow \pi/2. \end{aligned} \tag{2.22}$$

For $\kappa_B \geq 4$ the untwisted bipolar drop is preferred; for $\kappa_B \geq \frac{4}{3}$ there is part untwisted (small η) and part with $\tau = \pi/2$; and for $\kappa_B \leq \frac{4}{3}$, there is twist for all $\eta \geq 0$, with $\tau = \pi/2$ for the larger values.

We shall now investigate the response of the drop to a weak magnetic field. The nematogen molecules tend to line up parallel to the field, so we expect the untwisted drop to have its axis parallel to the field and the limiting toroidal drop to have its axis normal to the field. If the field is not weak, the director field will be distorted, and in the toroidal case lose axial symmetry, so that all the analysis of this paper would be invalid. We would, however, expect a second-order transition to be associated with the loss of axial symmetry, and we shall calculate the transition line in the weak field case.

The energy density associated with the magnetic field is proportional [8] to $(\mathbf{n} \cdot \mathbf{B})^2$, and for axisymmetric drops, we find that the axis is parallel to the field if

$$\begin{aligned} \frac{1}{3} &\leq V^{-1} \int dV (\mathbf{n} \cdot \hat{\mathbf{x}})^2 \\ &= 3 \int_0^{\pi/2} d\xi \int_0^{\pi/2} d\eta h_\xi h_\eta h_\phi \frac{(\sin \xi + \cos \eta)^2}{Z^4} \cos^2 \tau(\eta) \end{aligned} \tag{2.23}$$

where Z is from (2.12) and $h_\xi h_\eta h_\phi$ is the volume element from (2.13). This quantity is the average of the square of the component of \mathbf{n} along the axis: for the untwisted drop with $\tau = 0$ it is $\frac{79}{150}$, so the axis is parallel to the field, as observed experimentally [5]. For the toroidal drop $\tau = \pi/2$ and the average is zero, so the drop axis is normal, as surmised above.

3. Calculation

The Euler-Lagrange equation (2.17) is of boundary-layer type near $\eta = 0$, which is caused by the small quantity η multiplying the highest derivative. We can remove this singularity by transforming to the independent variable $y = \ln(2\eta/\pi)$ so that

$$\frac{d^2\tau}{dy^2} = \eta^2 \frac{d^2\tau}{d\eta^2} + \eta \frac{d\tau}{d\eta}. \quad (3.1)$$

The boundary conditions for $\tau(\eta)$ are now

$$\frac{d\tau}{dy}(y=0) = 0 \quad (3.2a)$$

$$\tau(y \rightarrow -\infty) = 0. \quad (3.2b)$$

We directly minimise the energy $u[\mathbf{n}]$ by the method of successive over-relaxation [13]. First we choose a large negative number y_{\min} and discretise the interval $(y_{\min}, 0)$ with spacing h . The energy is then quadratic in the discretised values τ_i and we cycle through these points, adjusting τ_i to minimise the energy locally. This process is completely equivalent to the numerical solution of the diffusion-like equation of Euler-Lagrange form:

$$\frac{\partial \tau}{\partial t} = -\frac{\partial F}{\partial \tau} + \frac{\partial}{\partial y} \frac{\partial F}{\partial \tau'}. \quad (3.3)$$

We find that the energy decreases monotonically to a limit, and we use the convergence criterion that the change in each τ_i per step should be less than 10^{-4} rad. We then make y_{\min} more negative and repeat the relaxation. This is continued until a further decrease in y_{\min} makes no difference within the above criterion.

In figure 3 we show a perspective view of a droplet with the director represented by small cylinders. The twisted appearance of the surface is similar to figure 2(b).

The solution $\tau(\eta)$ can be characterised by the elastic energy $u[\mathbf{n}]$, the exterior twist angle $\tau(\eta = \pi/2)$ and the initial slope $d\tau/d\eta(\eta = 0)$; these are shown in figures 4, 5 and 6, respectively, as contour plots in the (κ_B, κ_T) plane. In each of these figures, the most obvious feature is the curve joining $\kappa_T = 1, \kappa_B = 0$ to $\kappa_T = 0, \kappa_B = 4$, which is the second-order parity breaking transition from untwisted to twisted droplets. When κ_T is large, the condition (2.20) is a good approximation: the broken line in the figures is the continuation of that straight line. When κ_T is zero, the analysis (2.22) indicates that $\kappa_B = 4$ is a transition point: this is marked in the figures. The planar part of the energy surface in figure 4 is the exact expression (2.18) and the energy is zero at $\kappa_B = 0, \kappa_T = 0$ because this is the limiting toroidal case $\tau = \pi/2$ which has no splay energy.

In figure 6 the slope of $\tau(\eta)$ at $\eta = 0$ is plotted. When this is large the twist angle rises sharply to $\pi/2$ and stays there, so the director is azimuthal except near the axis, where there is a disclination. The width of this disclination is proportional to $\sqrt{\kappa_B}$

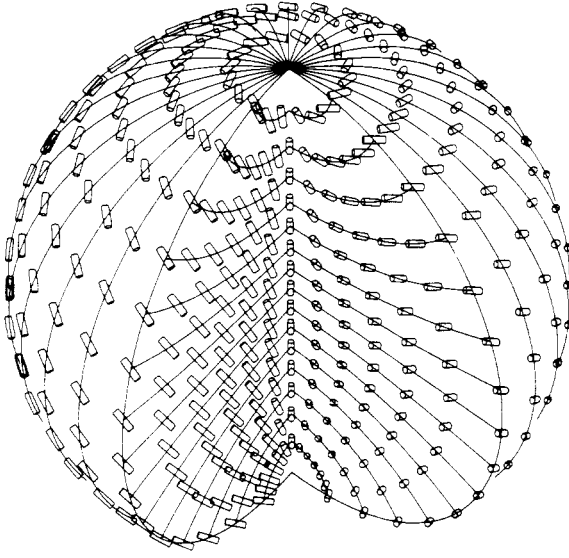


Figure 3. A perspective view of a droplet with a section removed to show the inside. The elastic constant ratios are $\kappa_B = 0.5$, $\kappa_T = 0.6$.

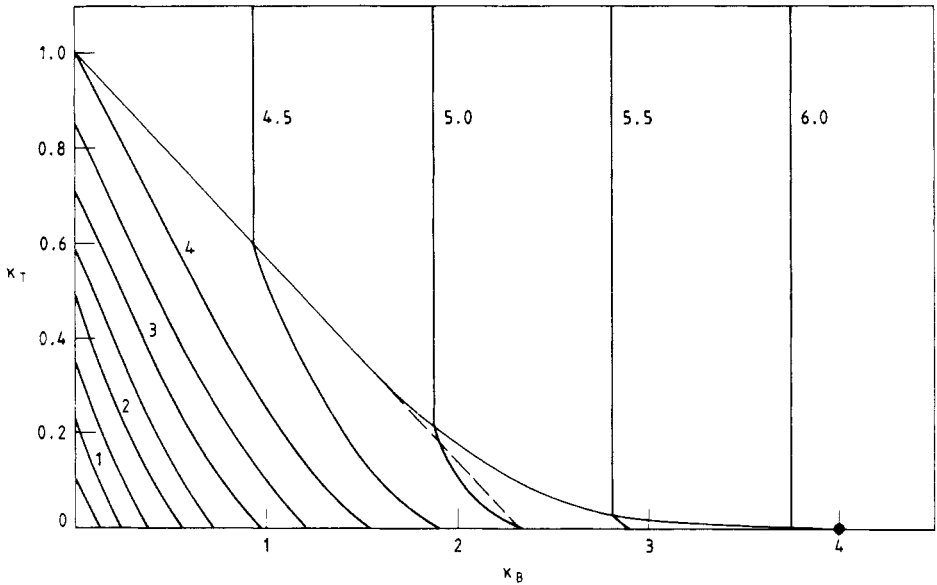


Figure 4. Dimensionless energy $u[n]$ as a contour plot in the plane $\kappa_B = K_{33}/K_{11}$, $\kappa_T = K_{22}/K_{11}$. The contour spacing is 0.5. The thin line is the phase transition line.

when κ_B is small. The surface twist angle in figure 5 is $\pi/2$ for small κ_B or small κ_T and has a square root singularity at the phase transition line.

We have calculated the double integral (2.23) by Simpson's rule with 50 points each way and the chain curve in figure 6 shows where it is $\frac{1}{3}$, and is the transition from the drop axis being parallel to normal (to a weak magnetic field).

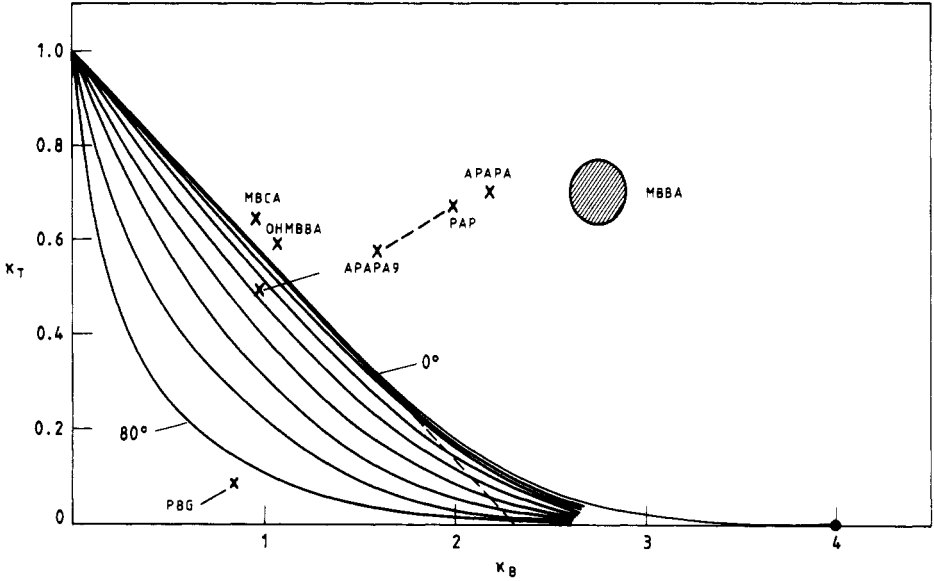


Figure 5. Contour plot of the surface twist angle $\tau(\eta)$ at $\eta = \pi/2$ with contour interval 10° . Data for some short-rod nematics are from [12]; the broken line for PAP is a temperature variation and the circle for MBBA is an error estimate.

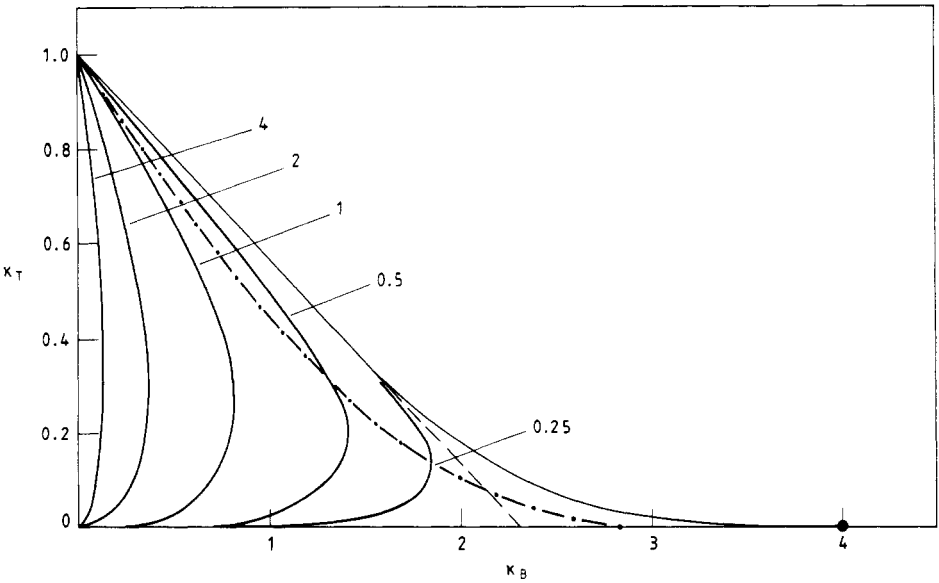


Figure 6. Contour plot of the internal twist $d\tau/d\eta$ at $\eta = 0$, which is the twist disclination strength at the axis.

Also marked on figure 5 are some experimental measurements of nematics [14]. All except one of these are short-rod nematics and one (PBG, poly- γ -benzyl-glutamate) is a polymer. These may not be tangentially anchored, although it is known that temperature [3], concentration and surfactant [10] can all change the anchoring angle. It is clear, however, that short-rod nematics generally lie outside the twisted region, although APAPA9 should be somewhat twisted. The measurement of the elastic constants of PBG is recent and bears out theoretical studies [12, 13] of elastic constants of nematic polymers. We predict that, if an interface prefers tangential anchoring, then PBG should exhibit highly twisted droplets.

4. Conclusions

We have taken a simple approximation to the elastic energy functional for a nematic droplet and shown that a transition to a twisted configuration occurs for large splay constant. While we do not expect our results to be quantitatively correct, in view of the approximation, it is reasonable to expect the main features to be qualitatively accurate. A treatment using the full elastic energy functional could be used to measure elastic constants, especially since some nematics will be just inside the twisted region, giving great sensitivity.

In a magnetic field, the director tends to align parallel to the field. For the untwisted drop, the axis must then be parallel, but for sufficiently large splay constant the axis is perpendicular. In this case the drop will cease to be axisymmetric, so we expect another transition. As above, any finite magnetic field will distort the drop and move the transition line, but the qualitative conclusion does not change.

Although elastic constants are available for only one polymer nematic, theoretical work [15] suggests that the relatively small K_{22} and K_{33} are generic features, so it would be interesting to observe droplets of polymer nematic to measure their twist characteristics, perhaps by polarised light scattering. The concentration of polymer affects the elastic constants and these twisted drops would be a good way of observing such variation.

It should be emphasised that the results of this paper are based on two assumptions. The first is that the drops are large enough that volume effects dominate surface effects and the second is that based on figure 1, that the director always lies on a tactoid surface, which is a circular arc rotated about a non-diametric line. These assumptions, while somewhat special, are reasonable.

Appendix

Let $\mathbf{n}(\mathbf{x})$ be a unit vector field on a domain V (the inside plus surface of the drop) and $\mathbf{k}(\mathbf{x})$ a vector field on a subset $S \subset V$. S is the surface of the drop and \mathbf{k} the outward normal. We can write the surface energy as $f_0 + \frac{1}{2}(\mathbf{n} \cdot \mathbf{k})^2$ where f_0 is the isotropic part of the surface tension, which we henceforth ignore. The total energy is

$$u_\mu[\mathbf{n}] = u[\mathbf{n}] + \mu \int_S \frac{1}{2}(\mathbf{n} \cdot \mathbf{k})^2 dx \quad (\text{A1})$$

where u is the positive-definite Frank energy. We show that, when $\mu \rightarrow \infty$, the minimum of $u_\mu[\mathbf{n}]$ is the minimum of $u[\mathbf{n}]$ with the boundary condition $\mathbf{n} \cdot \mathbf{k} = 0$.

Define the functional u'_μ of a scalar field, $\eta(x)$, $x \in S$, as

$$u'_\mu[\eta] = \min_{\mathbf{n} \cdot \mathbf{k} = \eta} u[\mathbf{n}] \quad (\text{A2})$$

which is the minimum of the Frank energy when $\mathbf{n} \cdot \mathbf{k} = \eta$ is specified on S . We assume that u' is sufficiently smooth that orthonormal real eigenfunctions $Q_i(x)$ exist on S so that if

$$\eta(x) = \sum_i \eta_i Q_i(x) \quad (\text{A3})$$

then

$$u'[\eta] = u'[0] + \sum p_i \eta_i + \sum \frac{1}{2} q_i \eta_i^2 + O(\eta^3). \quad (\text{A4})$$

Note that the q_i are bounded below because $u[\mathbf{n}]$ is positive-definite. We can now write

$$\begin{aligned} \min_{\mathbf{n}(x)} u_\mu[\mathbf{n}] &= \min_{\eta_i} \left(u'[0] + \sum p_i \eta_i + \sum \frac{1}{2} (q_i + \mu) \eta_i^2 + \dots \right) \\ &= u'[0] - \sum \frac{p_i^2}{2(q_i + \mu)} + \dots \end{aligned} \quad (\text{A5})$$

so that

$$\lim_{\mu \rightarrow \infty} \min_{\mathbf{n}(x)} u_\mu[\mathbf{n}] = u'[0] \quad (\text{A6})$$

which is the minimum Frank energy subject to the boundary condition $\mathbf{n} \cdot \mathbf{k} = 0$ on S .

References

- [1] Faetti S and Palleschi V 1984 *Phys. Rev. A* **30** 3241; 1985 *J. Physique* **46** 415
- [2] Press M J and Arrott A S 1974 *Phys. Rev. Lett.* **33** 403; 1975 *J. Physique* **36** C1 177
- [3] Volovik G E and Lavrentovich O D 1983 *Zh. Eksp. Teor. Fiz.* **85** 1997 (1984 *Sov. Phys.-JETP* **58** 1159)
Kurik M J and Lavrentovich O D 1982 *Zh. Eksp. Teor. Fiz. Pis. Red.* **35** 362 (*JETP Lett.* **35** 444)
- [4] Chandrasekhar S 1965 *Liquid Crystal Conf. Kent, Ohio, 1965* (New York: Gordon and Breach) p 261
- [5] Dubois-Violette E and Parodi O 1969 *J. Physique* **30** C4 57
- [6] Nehring J and Saupe A 1971 *J. Chem. Phys.* **54** 337
Ericksen J L 1976 *Adv. Liquid Cryst.* **2** 233
- [7] Jenkins J T and Barrett P J 1974 *Q. J. Mech. Appl. Math.* **27** 111
- [8] de Gennes P G 1974 *The Physics of Liquid Crystals* (Oxford: Oxford University Press)
- [9] Madhusudana N V and Sumathy K R 1983 *Mol. Cryst. Liquid Cryst. Lett.* **92** 179
- [10] Candau S, le Roy P and Debeauvais F 1973 *Mol. Cryst. Liquid Cryst.* **23** 283
- [11] Williams R D 1985 *Rutherford Appleton Laboratory Rep.* RAL-85-028
- [12] Meyer R B 1982 *Polymer Liquid Crystals* ed A Ciferri, W R Krigbaum and R B Meyer (New York: Academic) ch 6
- [13] Milne W E 1970 *Numerical Solution of Differential Equations* (New York: Dover)
- [14] Taratuta V G, Hurd A J and Meyer R B 1985 *Phys. Rev. Lett.* **55** 246
Miraldi E, Trossi L and Taverna Valabrega P 1981 *Nuovo Cimento B* **66** 179
Leenhouts F, Dekker A J and de Jeu W H 1979 *Phys. Lett.* **72A** 155
Gruher H 1973 *Z. Naturf.* **28a** 474
Leenhouts F and Dekker A J 1981 *J. Chem. Phys.* **74** 1956
- [15] de Gennes P G 1982 *Polymer Liquid Crystals* ed A Ciferri, W R Krigbaum and R B Meyer (New York: Academic) ch 5